

Ins-HOI: Instance Aware Human-Object Interactions Recovery

Jiajun Zhang¹, Yuxiang Zhang², Hongwen Zhang², Boyao Zhou², Ruizhi Shao²,
Zonghai Hu¹, Yebin Liu²

¹ Beijing University of Posts and Telecommunications ² Tsinghua University

Abstract

Recovering detailed interactions between humans/hands and objects is an appealing yet challenging task. Existing methods typically use template-based representations to track human/hand and objects in interactions. Despite the progress, they fail to handle the invisible contact surfaces. In this paper, we propose Ins-HOI, an end-to-end solution to recover human/hand-object reconstruction via instance-level implicit reconstruction. To this end, we introduce an instance-level occupancy field to support simultaneous human/hand and object representation, and a complementary training strategy to handle the lack of instance-level ground truths. Such a representation enables learning a contact prior implicitly from sparse observations. During the complementary training, we augment the real-captured data with synthesized data by randomly composing individual scans of humans/hands and objects and intentionally allowing for penetration. In this way, our network learns to recover individual shapes as completely as possible from the synthesized data, while being aware of the contact constraints and overall reasonability based on real-captured scans. As demonstrated in experiments, our method Ins-HOI can produce reasonable and realistic non-visible contact surfaces even in cases of extremely close interaction. To facilitate the research of this task, we collect a large-scale, high-fidelity 3D scan dataset, including 5.2k high-quality scans with real-world human-chair and hand-object interactions. We will release our dataset and source codes. Data examples and the video results of our method can be found on the project page: <https://jiajunzhang16.github.io/ins-hoi>.

1. Introduction

Human/hand object interactions (HOI) have significant applications in the fields of computer vision, robotics, and virtual reality. Accurately reconstructing the state of interaction enables a comprehensive understanding, analysis, and generation of human behavior. There is remarkable progress in separately reconstructing human [24, 31, 37,

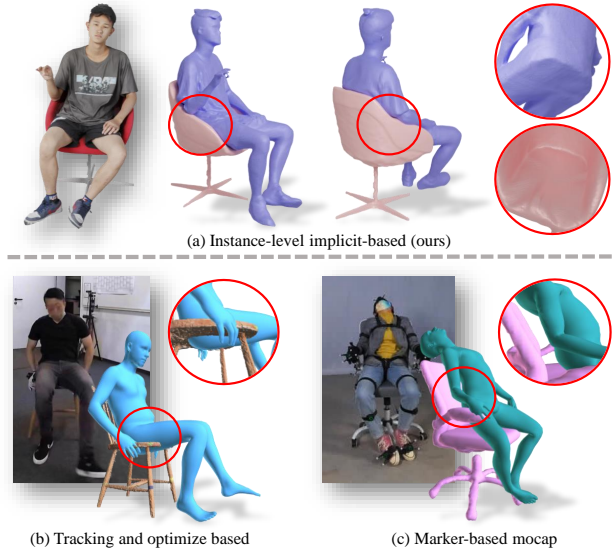


Figure 1. Our instance-level implicit-based approach achieves accurate reconstruction of the geometry and non-visible contact areas. In contrast, tracking and optimization-based methods [1], as well as marker-based methods [12] techniques, rely on human parametric template and present inaccuracies in interaction region and lack fine-detailed geometry.

38, 45], hand [8, 9, 14] and objects [2, 13, 27]. However, these methods are designed to reconstruct individual object and do not support the simultaneous reconstruction of two interacting instances. To overcome this limitation, numerous datasets and reconstruction methods [1, 6, 12, 18, 33, 39, 42] have been specifically developed for human/hand-object interactions. While these methods achieve reasonable results, they struggle to capture the intricate geometry and plausible non-visible surfaces.

A major limitation of previous HOI recovery solutions is that the template-based representations are employed to track the human/hand and objects in interactions. For instance, the parametric models like SMPL[20, 28] and MANO [30] are used to represent the human/hand poses, while pre-defined templates [36] are selected as the object representations. Constrained by the expressive power of

template-based representations, these methods exhibit limited capabilities as they are unable to reconstruct clothing or the fine deformations caused by contact, nor can they address issues of model penetration, as shown in Fig. 1. Regarding the interacting objects, most previous works assume the objects to be rigid, reconstructing them by simply tracking the pose of object templates [7, 42, 43]. This simplification of human/hand and object representations falls short in effectively handling the contact surfaces, which are crucial for accurately reconstructing close interactions.

Diverging from previous template-based solutions, we would argue for a more suitable HOI modeling paradigm by introducing instance-level human/hand-object reconstruction via implicit surface representations. The implicit representations are characterized by their continuous property, high-resolution details, and robustness to topological variations, which is more suitable to model the intricate geometric appearance and non-visible contact surfaces of the two interacting instances. Based on implicit representations, we present Ins-HOI, an end-to-end approach for human/hand-object interaction recovery at the instance level. As previous methods [25, 31] typically reconstruct the target scene as a single entity, the existing implicit field can not model distinct instances simultaneously. To handle this issue, we extend the implicit function by proposing an instance-level occupancy field to learn separate geometry for each instance. Such an extension not only allows our representation to support instance-aware perception but also enables a more direct constraint between the contact surfaces of different instances in our algorithm. Such a representation also allows our method to learn contact priors implicitly from sparse multi-view observations.

Though our representation is well-suited for instance-level reconstruction, achieving this goal is still non-trivial as it is challenging to acquire individual instance-level ground truth for two tightly interacting objects in real-world data. To address this issue, we propose a complementary training strategy to enhance the learning of individual geometric priors and the perception of interaction. Alongside real-scanned scans, we augment our training data with synthesized data. These are created by randomly composing human/hand scans with object scans, and intentionally allowing for some extent of penetration. These synthesized data have their ground truth instance shape (penetration areas are assigned to both human/hand and object) to make the network better learning the individual shape as completely as possible even under extremely closely interacting and occluded scenarios. For the real scans, it serves as a penalization to make our instance reconstructions share no penetration and assure seamless integration with the original real scans. Overall, the two types of data play adversarial and complementary roles in the training process. The synthesized data focuses on the completeness of individual

shapes, while the real-captured scans concentrate more on overall reasonableness.

In this paper, we demonstrate that Ins-HOI can handle two of the most common interaction scenarios: human-chair and hand-object interactions. Compared with previous implicit methods [31, 32], Ins-HOI achieves comparable reconstruction results when considering the interacting human/hand and objects as a whole. In addition, Ins-HOI can produce reasonable and realistic non-visible contact surfaces even in cases of extremely close interaction. Besides, our method requires only one forward pass, eliminating the need for tracking, modeling, and registration processes typically required by other HOI reconstruction methods [1, 12, 40, 42]. We hope our proposed method and datasets for instance-level human/hand-object recovery can pave the way for new research direction.

Our contributions can be summarized as follows:

- We propose instance-level human/hand-object reconstruction via implicit surface representations for the task of human/hand-object interaction. Our method learns the contact prior implicitly and produces reasonable and realistic non-visible contact surfaces even in cases of extremely close interaction.
- We propose a complementary training strategy to tackle the lack of instance-level ground truth in real-scanned datasets. Such a strategy can well balance the completeness of individual shapes and the overall reasonability of invisible contacts.
- We collect a large-scale, high-fidelity 3D scan dataset of human/hand-object interactions, named Ins-Sit and Ins-Grasp, comprising a total of 5.2k scans. We benchmark the task of instance-level reconstruction on our dataset.

2. Related Work

Human Object Interactions Recent studies [1, 10, 33, 43] explore human-object interactions via several constraints, such as contacts and spatial arrangement. These methods often represent the human form using parametric models [20, 28] and rely on pre-obtained object. However, the ideal representation of the human would have detailed geometry rather than relying on parametric model, which fall short in simulating the clothes, the deformation of muscle tissue under pressure. Likewise, objects represented by pre-scanned template cannot effectively model the deformations caused by contact. Several studies [40, 42] have utilized techniques such as NeRF [11, 35] and implicit avatars [5] to model human. However, the setup for these capture system is heavy and requires individual model training for each subject. Although these methods can achieve high fidelity, their deployment in real-world scenario remains challenging.

In this work, we aim to explore the intricate, instance-level reconstructions of human and objects, along with the

realistic contact surface deformations. As a testbed for our methods, we conducted experiments in the frequently encountered scenario of human-chair interactions. To our knowledge, COUCH [44] and CHAIRS [12], have investigate interactions between humans and chairs. However, both of these datasets focus on dynamic motions, which are captured through marker-based motion capture systems. They are unable to capture fine-grained geometry like casual suit and are not well suited for visual tasks due to the markers attached to the human body. Our Ins-Sit dataset, in contrast, captures static poses, allowing us to focus on things like texture or geometry of people’s clothes, and details when human interact with chair. Static scans and dynamic motion sequences are mutually complementary.

Hand Object Interactions Existing hand object interaction related datasets [7, 8, 18, 39] are constructed using multi-view setups to capture RGB sequences. The standard pipeline involves tracking the human hand and fitting it with parametric model [19, 30], while the interacting objects [36] are represented with pre-scanned models, with their poses being estimated subsequently. These datasets generally lack the capability to capture texture scans, leaving a gap in achieving realistic representation of surface deformation and textures due the inherent limitations of parametric model, which lacks of geometric detail and textural information. Although some efforts [19, 29] have been made to generate textures for parametric model, their fidelity still falls short when compared with real-world captured data.

In this work, to validate the feasibility of our instance-level reconstruction method for hand-object scenarios, we also captured a collection of hand-object interaction scans, named Ins-Grasp. This dataset fills the existing gap in textured scan data of hand-object interactions within the research community.

3. Dataset

The existing high-fidelity 3D geometry datasets tend to have a limited scope, focusing on either humans [23, 41], hands [7, 39] or objects [4] individually. Motion capture and optimization-based dataset for human object interaction often rely on parametric templates, which lack the intricate geometry and contact details. This limitation hinders more in-depth research on human/hand-object interactions, especially in cases of close interactions. To bridge this gap, we create a new dataset named Ins-Sit and Ins-Grasp for human-chair and hand-object interactions, respectively. Moreover, we also augment our dataset by synthesizing data based on existing individual human/hand and object scans.

3.1. Real-scanned Data

Our proposed dataset comprises two parts: hand-object interactions and human-chair interactions, as illustrated in the



Figure 2. Examples of high-fidelity, textured 3D scans from Ins-Sit and Ins-Grasp.

Fig. 2. Our capture system consists of 128 DSLR cameras arranged uniformly in a sphere and the captured images are reconstructed using commercial software. For human-chair interactions, the proposed Ins-Sit dataset comprises a total of 4700 scans, involving 72 subjects (12 females and 60 males). Each subject seated on 2 of 11 distinct chair types and perform 60 unique poses. We fit SMPL-X [28] to human part in our scan through keypoints estimated from dense-view rendered images [3, 22]. We also annotate the semantic label of each vertex in the scan by employing a combination of SAM [16] and multi-view fusion [17] techniques for potential research purposes. In the context of human-chair interactions, the pose and clothing of the subjects significantly influence the reconstruction results.

For hand-object interactions, the proposed Ins-Grasp dataset emphasizes more on the diversity of the objects. We collected data on 50 different objects, each involved in 10 distinct interactions. There are 20 volunteers participating in the data acquisition, contributing to a collection of 500 scans. We also fit MANO [30] and NIMBLE [19] with the same procedure as human-chair interactions for potential purposes.

3.2. Synthetic Data Augmentation

The real-scanned dataset provides the interaction information as a single, connected mesh, which lacks individual ground truths. Although we can segment surface with the combination of image segmentation [16] and multi-view fusion [17] techniques, it is still impossible to recover the invisible contact area reasonably, as shown in supplementary materials. To support the learning of individual shape for our network, we leverage individual scans of human, hand, and objects to generate synthetic data.

For human-chair interactions, we take a human scan H_p from the existing high-quality human scans THuman2.0 [41] and couple it with an individual chair scan C to imitate human-chair interactions, as shown in Fig. 3(a). As the subjects in THuman2.0 [41] are mostly scanned under

standing poses, we further repose the human scans based on a sited poses randomly selected from our real-scanned data. To do so, we first apply the inverse LBS (Linear Blend Skinning) procedure to transform H_p to T-pose as H_p^0 . We then generate the reposed SMPL-X parameters θ_r by integrating the upper body pose of θ_p and the lower body pose of θ_q . Next, we obtain the driven mesh of H_p in pose θ_r as H_r , *i.e.*,

$$\begin{cases} H_r = \mathcal{M}(\mathcal{M}^{-1}(H_p, \theta_p, W_{H_p}), \theta_r, W_{H_p}) \\ \theta_r = \text{concat}(\{\theta_p^i | i \in \text{upperbody}\}, \{\theta_q^i | i \in \text{lowerbody}\}) \end{cases} \quad (1)$$

where \mathcal{M} denotes the LBS function, then W_{H_p} is the LBS weight of H_p . For each vertex in H_p , we simply take the weight of the nearest SMPL-X vertex in practice. Based on the standing and reposed humans and chairs, we arrange these scans in 3D space by allowing for a random extent of penetration. Overall, for human-chair interactions, our synthetic data comprises two types: standing and reposed sitting humans, denote as Syn_s and Syn_r, respectively.

The similar synthetic strategy is also used to generate the augment data for hand-object interactions. As the hand in grasping poses can be easily scanned in our system, we couple individual hand scans with objects directly the without reposing the hand scans.

4. Method

Given only sparse view images as input, our method Ins-HOI supports instance-level implicit reconstructions of two interacting objects, and recovers plausible contact surfaces in non-visible areas. Ins-HOI is a unified method for both human-object and hand-object interactions. For clarity, we illustrate the pipeline of our method based on human-chair interactions, as shown in Fig. 3.

In this section, we first introduce the proposed instance-level implicit functions (Sec. 4.1), then the complementary training strategy (Sec. 4.2).

4.1. Instance-level Neural Surface Field

Our representation is built upon the pixel-aligned implicit functions [31], which defines a surface as a level set as follows:

$$f(F(x), \pi(X), z(X)) = s, s \in [0, 1], \quad (2)$$

where $x = \pi(X)$ represents the projected 2D point in the image plane from the given 3D point X , $Z(X)$ denotes the depth value from X to the camera, and $F(x)$ represents the pixel-aligned feature at x . Inspired by [32], we further introduce a position embedding γ and a view direction $d(x)$ as extra input features. The above pixel-aligned implicit functions only represent the target object as a single entity. For instance-level reconstruction, we extend the implicit functions to support simultaneous representation of human/hand

and objects. Specifically, the proposed instance-level occupancy field has different outputs corresponding to human/hand and object as follows:

$$\begin{cases} f_H(F(x), \gamma(d(x))) = s_H, s_H \in [0, 1] \\ f_O(F(x), \gamma(d(x))) = s_O, s_O \in [0, 1] \end{cases} \quad (3)$$

Here, s_H and s_O refer to the occupancy fields of the human body and the chair, respectively. The human/hand mesh is represented by $H = \{X | f_H(X) = 1\}$, and the object mesh by $O = \{X | f_O(X) = 1\}$.

Based on the proposed implicit human/hand and object representation, we can obtain their union and their intersection as follows:

$$\begin{aligned} U &= \{X | f_H(X) = 1 \text{ or } f_O(X) = 1\} \\ &= \{X | \max(f_H(X), f_O(X)) = 1\} \end{aligned} \quad (4)$$

$$\begin{aligned} I &= \{X | f_H(X) = 1 \text{ and } f_O(X) = 1\} \\ &= \{X | f_H(X) \cdot f_O(X) = 1\} \end{aligned} \quad (5)$$

An example output of the instance-level occupancy field is shown in Fig. 4, where their union and intersection are also visualized for better illustration.

Based on our representation, we can directly supervise the union and penalize the intersection of two interacting objects. For inference, we reconstruct the meshes by densely sampling the occupancy field s_H and s_O respectively over the 3D space and extract the iso-surface at threshold 0.5 using the Marching Cube algorithm [21].

4.2. Supplementary Training

Based on the real-scanned and synthesized data described in Sec. 3.2, we further introduce a supplementary training strategy for instance-level human-object recovery. During the supplementary training, our network leverages the two types of training data, namely the synthetic data $\{\text{Syn}_s, \text{Syn}_r\}$ and real-scanned data $\{U_q\}$ as described in Sec 3.

The synthetic data comprises the information of individual human/hand H_p and the chair C , which offers strong guidance for the learning of human and chair implicit functions $f_H(X)$ and $f_C(X)$:

$$\mathcal{L}_i = \frac{1}{n} \sum_{i=1}^n (|f_H(X) - f_H^*(X)|^2 + |f_C(X) - f_C^*(X)|^2) \quad (6)$$

The real-scanned data is taken from the proposed Ins-Sit scan dataset. Due to the lack of instance-level ground truth, direct supervision of the individual human/hand and object is not feasible. As the real-scanned data offers actual interaction information in the form of unified human-chair and hand-object meshes, we leverage such data by imposing supervision on the unioned implicit function and penalty on their intersection. Specifically, the supervision on the union

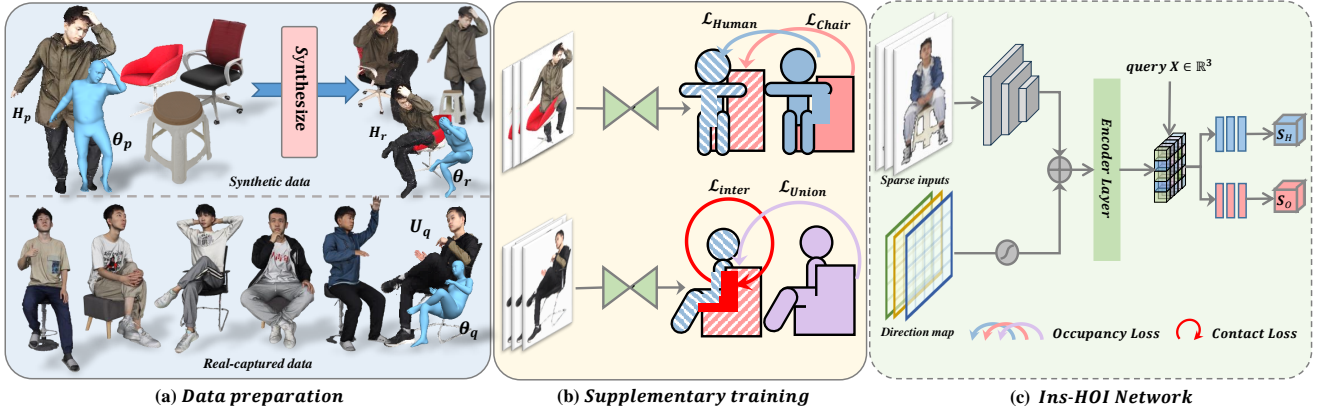


Figure 3. Overview of the method: (a) showcases the synthetic data augmentation process using THuman and Ins-Sit dataset to form a training dataset. (b) highlights how the training components provide unique guidance for complementary learning (blue and pink denote the human and chair meshes; purple and red indicate the union and intersection). (c) depicts our benchmark Ins-HOI, which given sparse view inputs to produce instance-level human-object recovery via an end-to-end approach.

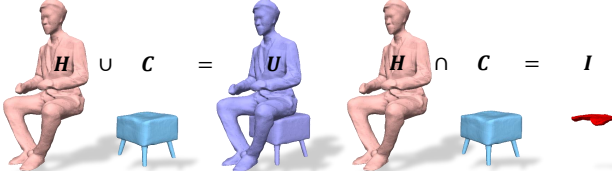


Figure 4. Example of Union and Intersection operation under our definition.

surface enhances the reconstruction of the interacting human/hand and objects as a whole, where the learning objective is defined based on $f_U(X) = \max(f_H(X), f_C(X))$:

$$\mathcal{L}_u = \frac{1}{n} \sum_{i=1}^n |\max(f_H(X), f_C(X)) - f_U^*(X)|^2 \quad (7)$$

In addition, the penalty on the intersection $I = H \cap C$ encourages an empty set, such that the predicted human/hand and object meshes are separated from each other:

$$\mathcal{L}_{in} = \frac{1}{n} \sum_{i=1}^n \max(0, f_H(X) - 0.5)^{1-\gamma} \cdot \max(0, f_C(X) - 0.5)^\gamma \quad (8)$$

Here γ is introduced as a hyper-parameter to control the rigidity of the objects. For instance, when γ is set to 1, the gradient $\frac{\partial \mathcal{L}_{in}}{\partial f_H}(X)|_{\gamma=1} \equiv 0$, which means that only the object occupancy $f_C(X)$ is penalized to prevent intersection, resulting a more completed object without deformation. Conversely, when γ is set to 0, only the human occupancy $f_H(X)$ is penalized to allow more intensive deformation of the objects. In practice, we annotate the value of γ for different types of chairs and objects in our Ins-HOI dataset. This allows us to inject the knowledge of chair materials and control the degree of deformation when a per-

son is seated, which will be further discussed in our experiments. In summary, the entire training objective can be written and minimized as:

$$\mathcal{L}_{total} = \mathcal{L}_i + \mathcal{L}_u + \mathcal{L}_{in} \quad (9)$$

5. Experiments

Ins-Sit and Ins-Grasp datasets serve multiple purposes, enabling 3D reconstruction, novel view synthesis, motion capture, motion generation, etc. We benchmark our dataset on reconstruction tasks in this paper. Due to the manuscript length constraint, we primarily details experiments on Ins-Sit. Details of the hand-object experiments will be presented in the appendix.

5.1. Datasets and Evaluation metrics

We partitioned 4,700 human-chair interaction scans into 4,000 for training and 700 for testing. The test set is further divided into two subsets: a cross-subject subset comprising individuals not encountered during training, and a within-subject subset containing known individuals but in new poses. For evaluation, we take cues from well-regarded research on clothed human reconstruction [31, 38, 45]. Following them, we leverage Chamfer Distance and Point-to-Surface as our key metrics.

5.2. Benchmark on Geometry Reconstruction

In contrast to the instance-level reconstruction introduced in our paper, existing reconstruction methods typically yield a single connected mesh, which we denoted as holistic reconstruction. We have trained the well-established PIFu [31], DoubleField [32] and NeuS2 [34] to establish a benchmark for reconstruction tasks. The first two methods are based on implicit function, while the latter, NeuS2 is based on neural



Figure 5. Qualitative comparison with PIFu [31], DoubleField [32] and NeuS2[34] on Ins-Grasp dataset.

rendering. For instance-level reconstruction, our approach is constrained by the absence of instance-level ground truth data for both training and evaluation. To address this, we merge the two instances and compared the unified outer surface of combined meshes against the holistic mesh. We then measure the intersection between two instances to demon-

strate the accuracy and plausibility of our reconstruction. All the experiments are conducted under same settings, with image resolution of 512x 512 and 6 input views.

To assess the quality of our reconstruction, we evaluate it in two-fold. Quantitatively, as illustrate in Tab. 1, Ins-HOI achieves comparable performance despite the ab-

sence of direct supervision. Ins-HOI surpasses PIFu and is slightly worse than DoubleField, but uniquely supports instance-level reconstruction. It is noteworthy that our results exhibit better accuracy under the cross-subject setting than within-subject, an observation that may seem counter-intuitive. This can be primarily attributed to the fact that the influence of pose variation on reconstruction is more pronounced than the identity of the subject. Within the Ins-Sit dataset, we selected 6 out of 72 subjects for cross-subject testing and used the remaining 66 for within-subject testing, with each subject contributing 5 random poses, this selection of identity may introduce extent of randomness.

Qualitatively, as demonstrated in Fig. 5, our reconstruction results are visually superior to those of PIFu, NeuS2 and comparable with DoubleField. Additionally, our method can achieve plausible and realistic results of non-visible contact surfaces with non-rigid deformations.

Overall, the reconstructed geometry has been evaluated in both quantitatively and qualitatively way. Additionally, for the non-visible contact surfaces, we also evaluated the degree of intersection between the two instances in Tab. 2. The results demonstrate that we achieved notably low penetration and Intersection over Union (IoU), indicating that our reconstruction of contact regions closely approximates the actual ground truth.

Methods (6 views)	Cross-subject		Within-subject		Instance Level
	Chamfer ↓	P2S ↓	Chamfer ↓	P2S ↓	
PIFu	0.5192	0.5246	0.5320	0.5760	✗
DoubleField	0.4637	0.4384	0.4616	0.4397	✗
Ours	0.4726	0.4578	0.4833	0.4763	✓

Table 1. Quantitative comparison of 3D reconstruction methods on the Ins-Sit dataset. We evaluates the performance of each method using Chamfer distance and Point-to-Surface (P2S) metrics (cm) and their capability at the instance level.

	Cross-subject		Within-subject		
	IoU(%) ↓	Volume(m^3) ↓	IoU(%) ↓	Volume(m^3) ↓	
w/o \mathcal{L}_{in}	8.1%	$8.59e^{-3}$	7.65%	$8.16e^{-3}$	
w/ \mathcal{L}_{in}	0.058%	$5.86e^{-5}$	0.055%	$5.56e^{-5}$	

Table 2. Quantitative evaluation of intersection degree with \mathcal{L}_{in} .

5.3. Ablation Study

Intersection constraint \mathcal{L}_{in} Despite the assistance of synthetic data in learning strong instance priors, without addressing the potential overlap of the two occupancy fields, the human is likely to intersect with the object in contact areas. In Tab. 2, we quantified the degree of intersection between the two reconstructed instances w/ and w/o intersection loss. In Fig. 6, we visualized the heat maps of intersection for both instances. It is clearly evident from our results that, with the contact constraints, the degree of mesh intersection is significantly reduced to minimal.

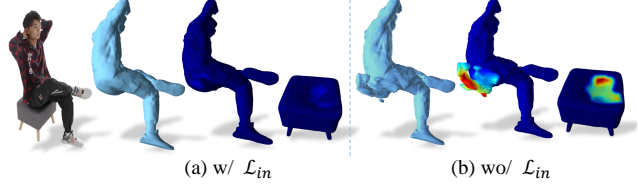


Figure 6. Qualitative evaluation of intersection constraint \mathcal{L}_{in} . We demonstrate the geometry and intersection heatmap in w/ and w/o \mathcal{L}_{in} in (a) and (b), respectively.

Prior intensity γ To better reconstruct the inner contact surfaces, drawing from both observed image features and intrinsic material properties, we introduce the hyper-parameter γ to guide network learning the extent of deformation. The impact of varying γ is depicted in Figure 7. With γ set to 0.5, an equitable balance in penalization is applied to both chairs and humans as detailed in Section 4.2, resulting in noticeable deformation of the chair. Conversely, γ value of 1 yields an flat, undistorted and smoother contact surface. The introduction of the γ coefficient makes the deformation of contact surfaces controllable, with a higher setting applied for rigid materials and a lower one for softer materials.

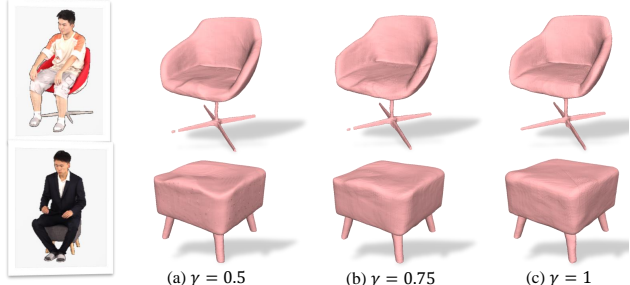


Figure 7. Ablation study of γ coefficient. Variation of γ control the penalization degree of human chair occupancy, thereby influence the extent of chair surface deformation.

Synthetic data augmentation As illustrated in Fig. 3, our complementary learning approach is facilitated by two types of data: synthetic and real-captured. The synthetic data is divided into two subcategories: one includes standing humans with chairs, denoted as Syn_S, and the other comprises reposed humans and chairs, denoted as Syn_R. Fig. 8 explains the contribution of each data category. As demonstrated in Fig. 8(a), without real-captured data, the network is unable to learn detailed geometry and constraints of intersection. Fig. 8(b) shows that without repose synthetic data Syn_R, the network struggles to learn a good prior for chairs due to a visual discrepancy between standing synthetic data and real data.

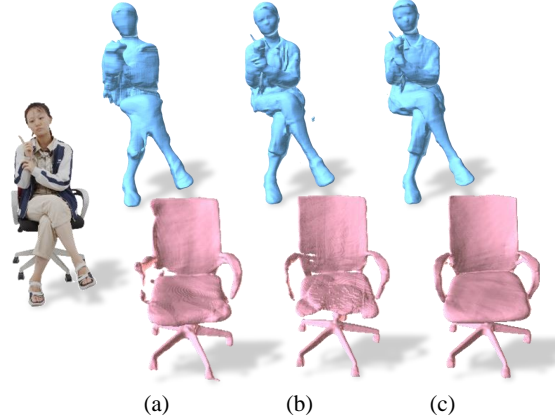


Figure 8. Ablation study on the contribution of dataset types: (a)-(b) show reconstructions without real-captured data and reposed data, respectively. (c) includes all dataset types, leading to the most comprehensive result.

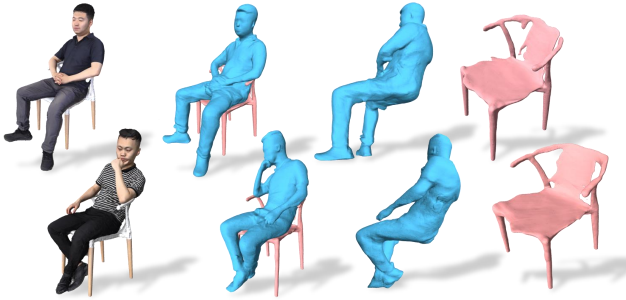


Figure 9. Experiments of fine-tuning on novel object, demonstrating that our model’s ability to generalize to new objects with limited synthetic data for fine-tuning by using 6 input views.

5.4. Fine-tune Experiments

To validate the generalization ability of our Ins-HOI, we conducted a fine-tuning experiment, as shown in Fig. 9. Since the model has been trained on our large-scale Ins-Sit, it has effectively learned the fine geometric priors of seated human poses. Therefore, when given a new type of chair, we synthesized 500 data by integrating chair model with scans from THuman [41], including both standing and reposed sitting pose. Approximately half an hour of fine-tuning is sufficient to achieve plausible results.

5.5. Hand-object interactions

Our proposed method is versatile, applicable not only to human-object interaction scenarios but also to hand-object interactions, enabling instance-level reconstructions with soft deformation on the contact surfaces. Due to manuscript length constraints, we present only a subset of results in Fig 10. Extensive experiments have been conducted on the publicly available HO-3D [7] dataset as well as on our own

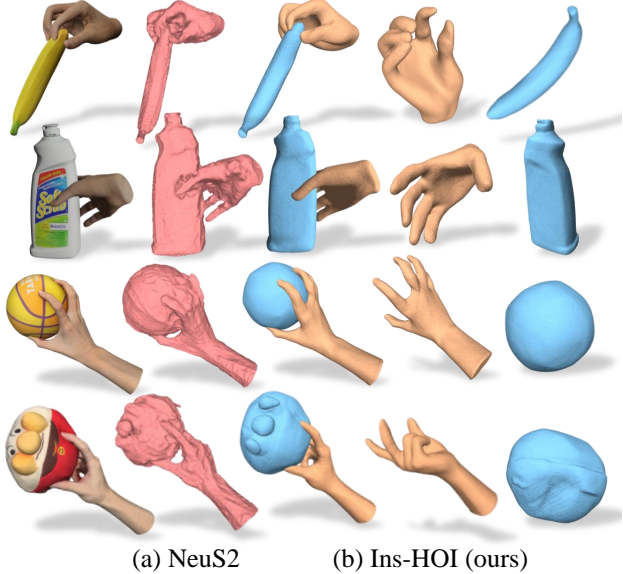


Figure 10. Qualitative results of instance-level reconstruction using our Ins-HOI method for hand-object interactions. Line 1-2 present results from HO-3D datasets, while Line 3-4 depict results from our Ins-Grasp dataset.

dataset. Here, we present a comparison between NeuS2 and Ins-HOI. For additional results and more details, please refer to the appendix.

6. Conclusion

In this work, we present Ins-HOI, the first end-to-end framework of instance-level reconstruction for human/hand-object interactions. To this end, we curated two comprehensive dataset, Ins-Sit and Ins-Grasp. Our methods established a robust and efficient benchmark, showcasing its ability to yield high-quality reconstructions along with plausible contact surfaces, that surpasses existing methods. In future work, our dataset and the proposed complementary learning approach could be integrated with newer 3D representations like NeRF [26] and Gaussian splatting [15], aims to reduce the number of input viewpoints for more efficient instance-level reconstruction.

Limitation While our method’s ability to recover contact regions has been validated through both qualitative and quantitative assessments, it is important to note that our results, albeit reasonable, are an approximation of ground truth. Accurately capturing true ground truth for contact deformation remains an exceedingly complex challenge. Additionally, our proposed model needs slight fine-tuning when introduced to a novel object type. This limitation could be mitigated by incorporating a more diverse range of objects.

References

- [1] Bharat Lal Bhatnagar, Xianghui Xie, Ilya Petrov, Cristian Sminchisescu, Christian Theobalt, and Gerard Pons-Moll. Behave: Dataset and method for tracking human object interactions. In *IEEE Conference on Computer Vision and Pattern Recognition (CVPR)*. IEEE, 2022. 1, 2
- [2] Alexandre Boulch and Renaud Marlet. Poco: Point convolution for surface reconstruction. In *Proceedings of the IEEE/CVF Conference on Computer Vision and Pattern Recognition (CVPR)*, pages 6302–6314, 2022. 1
- [3] Z. Cao, G. Hidalgo Martinez, T. Simon, S. Wei, and Y. A. Sheikh. Openpose: Realtime multi-person 2d pose estimation using part affinity fields. *IEEE Transactions on Pattern Analysis and Machine Intelligence*, 2019. 3
- [4] Angel X Chang, Thomas Funkhouser, Leonidas Guibas, Pat Hanrahan, Qixing Huang, Zimo Li, Silvio Savarese, Manolis Savva, Shuran Song, Hao Su, et al. Shapenet: An information-rich 3d model repository. *arXiv preprint arXiv:1512.03012*, 2015. 3
- [5] Xu Chen, Yufeng Zheng, Michael J Black, Otmar Hilliges, and Andreas Geiger. Snarf: Differentiable forward skinning for animating non-rigid neural implicit shapes. In *International Conference on Computer Vision (ICCV)*, 2021. 2
- [6] Zicong Fan, Omid Taheri, Dimitrios Tzionas, Muhammed Kocabas, Manuel Kaufmann, Michael J. Black, and Otmar Hilliges. ARCTIC: A dataset for dexterous bimanual hand-object manipulation. In *Proceedings IEEE Conference on Computer Vision and Pattern Recognition (CVPR)*, 2023. 1
- [7] Shreyas Hampali, Mahdi Rad, Markus Oberweger, and Vincent Lepetit. Honnotate: A method for 3d annotation of hand and object poses. In *CVPR*, 2020. 2, 3, 8
- [8] Yana Hasson, GÜl Varol, Dimitris Tzionas, Igor Kalevatykh, Michael J. Black, Ivan Laptev, and Cordelia Schmid. Learning joint reconstruction of hands and manipulated objects. In *CVPR*, 2019. 1, 3
- [9] Di Huang, Xiaopeng Ji, Xingyi He, Jiaming Sun, Tong He, Qing Shuai, Wanli Ouyang, and Xiaowei Zhou. Reconstructing hand-held objects from monocular video. In *SIGGRAPH Asia Conference Proceedings*, 2022. 1
- [10] Yinghao Huang, Omid Taheri, Michael J Black, and Dimitrios Tzionas. Intercap: Joint markerless 3d tracking of humans and objects in interaction. In *Pattern Recognition: 44th DAGM German Conference, DAGM GCPR 2022, Konstanz, Germany, September 27–30, 2022, Proceedings*, pages 281–299. Springer, 2022. 2
- [11] Zhang Jiakai, Liu Xinhang, Ye Xinyi, Zhao Fuqiang, Zhang Yanshun, Wu Minye, Zhang Yingliang, Xu Lan, and Yu Jingyi. Editable free-viewpoint video using a layered neural representation. In *ACM SIGGRAPH*, 2021. 2
- [12] Nan Jiang, Tengyu Liu, Zhexuan Cao, Jieming Cui, Yixin Chen, He Wang, Yixin Zhu, and Siyuan Huang. Full-body articulated human-object interaction. In *ICCV*, 2023. 1, 2, 3
- [13] Yue Jiang, Dantong Ji, Zhizhong Han, and Matthias Zwicker. Sdfdiff: Differentiable rendering of signed distance fields for 3d shape optimization. In *The IEEE/CVF Conference on Computer Vision and Pattern Recognition (CVPR)*, 2020. 1
- [14] Korrawe Karunratanakul, Jinlong Yang, Yan Zhang, Michael Black, Krikamol Muandet, and Siyu Tang. Grasping field: Learning implicit representations for human grasps. In *2020 International Conference on 3D Vision (3DV 2020)*, pages 333–344, Piscataway, NJ, 2020. IEEE. 1
- [15] Bernhard Kerbl, Georgios Kopanas, Thomas Leimkühler, and George Drettakis. 3d gaussian splatting for real-time radiance field rendering. *ACM Transactions on Graphics*, 42(4), 2023. 8
- [16] Alexander Kirillov, Eric Mintun, Nikhila Ravi, Hanzi Mao, Chloe Rolland, Laura Gustafson, Tete Xiao, Spencer Whitehead, Alexander C. Berg, Wan-Yen Lo, Piotr Dollár, and Ross Girshick. Segment anything. *arXiv:2304.02643*, 2023. 3
- [17] Abhijit Kundu, Xiaoqi Yin, Alireza Fathi, David Ross, Brian Brewington, Thomas Funkhouser, and Caroline Pantofaru. Virtual multi-view fusion for 3d semantic segmentation. In *Computer Vision–ECCV 2020: 16th European Conference, Glasgow, UK, August 23–28, 2020, Proceedings, Part XXIV 16*, pages 518–535. Springer, 2020. 3
- [18] Kailin Li, Lixin Yang, Haoyu Zhen, Zenan Lin, Xinyu Zhan, Licheng Zhong, Jian Xu, Kejian Wu, and Cewu Lu. Chord: Category-level hand-held object reconstruction via shape deformation. In *Proceedings of the IEEE/CVF International Conference on Computer Vision (ICCV)*, pages 9444–9454, 2023. 1, 3
- [19] Yuwei Li, Longwen Zhang, Zesong Qiu, Yingwenqi Jiang, Nianyi Li, Yuxin Ma, Yuyao Zhang, Lan Xu, and Jingyi Yu. Nimble: A non-rigid hand model with bones and muscles. *ACM Trans. Graph.*, 41(4), 2022. 3
- [20] Matthew Loper, Naureen Mahmood, Javier Romero, Gerard Pons-Moll, and Michael J. Black. SMPL: A skinned multi-person linear model. *ACM Trans. Graphics (Proc. SIGGRAPH Asia)*, 34(6):248:1–248:16, 2015. 1, 2
- [21] William E Lorensen and Harvey E Cline. Marching cubes: A high resolution 3d surface construction algorithm. *ACM siggraph computer graphics*, 21(4):163–169, 1987. 4
- [22] Camillo Lugaressi, Jiujiang Tang, Hadon Nash, Chris McClanahan, Esha Uboweha, Michael Hays, Fan Zhang, Chuo-Ling Chang, Ming Guang Yong, Juhyun Lee, Wan-Teh Chang, Wei Hua, Manfred Georg, and Matthias Grundmann. Mediapipe: A framework for building perception pipelines. *CoRR*, abs/1906.08172, 2019. 3
- [23] Qianli Ma, Jinlong Yang, Anurag Ranjan, Sergi Pujades, Gerard Pons-Moll, Siyu Tang, and Michael J. Black. Learning to Dress 3D People in Generative Clothing. In *Computer Vision and Pattern Recognition (CVPR)*, 2020. 3
- [24] Qianli Ma, Jinlong Yang, Siyu Tang, and Michael J. Black. The power of points for modeling humans in clothing. In *Proceedings of the IEEE/CVF International Conference on Computer Vision (ICCV)*, 2021. 1
- [25] Lars Mescheder, Michael Oechsle, Michael Niemeyer, Sebastian Nowozin, and Andreas Geiger. Occupancy networks: Learning 3d reconstruction in function space. In *Proceedings of the IEEE Conference on Computer Vision and Pattern Recognition*, 2019. 2
- [26] Ben Mildenhall, Pratul P. Srinivasan, Matthew Tancik, Jonathan T. Barron, Ravi Ramamoorthi, and Ren Ng. Nerf:

- Representing scenes as neural radiance fields for view synthesis. In *ECCV*, 2020. 8
- [27] Jeong Joon Park, Peter Florence, Julian Straub, Richard Newcombe, and Steven Lovegrove. DeepSDF: Learning continuous signed distance functions for shape representation. In *The IEEE Conference on Computer Vision and Pattern Recognition (CVPR)*, 2019. 1
- [28] Georgios Pavlakos, Vasileios Choutas, Nima Ghorbani, Timo Bolkart, Ahmed A. A. Osman, Dimitrios Tzionas, and Michael J. Black. Expressive body capture: 3D hands, face, and body from a single image. In *Proceedings IEEE Conf. on Computer Vision and Pattern Recognition (CVPR)*, pages 10975–10985, 2019. 1, 2, 3
- [29] Neng Qian, Jiayi Wang, Franziska Mueller, Florian Bernard, Vladislav Golyanik, and Christian Theobalt. HTML: A Parametric Hand Texture Model for 3D Hand Reconstruction and Personalization. In *Proceedings of the European Conference on Computer Vision (ECCV)*. Springer, 2020. 3
- [30] Javier Romero, Dimitrios Tzionas, and Michael J. Black. Embodied hands: Modeling and capturing hands and bodies together. *ACM Transactions on Graphics, (Proc. SIGGRAPH Asia)*, 36(6), 2017. 1, 3
- [31] Shunsuke Saito, Zeng Huang, Ryota Natsume, Shigeo Morigi, Angjoo Kanazawa, and Hao Li. Pifu: Pixel-aligned implicit function for high-resolution clothed human digitization. *arXiv preprint arXiv:1905.05172*, 2019. 1, 2, 4, 5, 6
- [32] Ruizhi Shao, Hongwen Zhang, He Zhang, Mingjia Chen, Yanpei Cao, Tao Yu, and Yebin Liu. Doublefield: Bridging the neural surface and radiance fields for high-fidelity human reconstruction and rendering. In *CVPR*, 2022. 2, 4, 5, 6
- [33] Omid Taheri, Nima Ghorbani, Michael J. Black, and Dimitrios Tzionas. GRAB: A dataset of whole-body human grasping of objects. In *European Conference on Computer Vision (ECCV)*, 2020. 1, 2
- [34] Yiming Wang, Qin Han, Marc Habermann, Kostas Daniilidis, Christian Theobalt, and Lingjie Liu. Neus2: Fast learning of neural implicit surfaces for multi-view reconstruction. In *Proceedings of the IEEE/CVF International Conference on Computer Vision (ICCV)*, 2023. 5, 6
- [35] Chung-Yi Weng, Brian Curless, Pratul P. Srinivasan, Jonathan T. Barron, and Ira Kemelmacher-Shlizerman. HumanNeRF: Free-viewpoint rendering of moving people from monocular video. In *Proceedings of the IEEE/CVF Conference on Computer Vision and Pattern Recognition (CVPR)*, pages 16210–16220, 2022. 2
- [36] Yu Xiang, Tanner Schmidt, Venkatraman Narayanan, and Dieter Fox. Posecnn: A convolutional neural network for 6d object pose estimation in cluttered scenes. 2018. 1, 3
- [37] Yuliang Xiu, Jinlong Yang, Dimitrios Tzionas, and Michael J. Black. ICON: Implicit Clothed humans Obtained from Normals. In *Proceedings of the IEEE/CVF Conference on Computer Vision and Pattern Recognition (CVPR)*, pages 13296–13306, 2022. 1
- [38] Yuliang Xiu, Jinlong Yang, Xu Cao, Dimitrios Tzionas, and Michael J. Black. ECON: Explicit Clothed humans Optimized via Normal integration. In *Proceedings of the IEEE/CVF Conference on Computer Vision and Pattern Recognition (CVPR)*, 2023. 1, 5
- [39] Lixin Yang, Kailin Li, Xinyu Zhan, Fei Wu, Anran Xu, Liu Liu, and Cewu Lu. OakInk: A large-scale knowledge repository for understanding hand-object interaction. In *IEEE/CVF Conference on Computer Vision and Pattern Recognition (CVPR)*, 2022. 1, 3
- [40] Yifei Yin, Chen Guo, Manuel Kaufmann, Juan Zarate, Jie Song, and Otmar Hilliges. Hi4d: 4d instance segmentation of close human interaction. In *Computer Vision and Pattern Recognition (CVPR)*, 2023. 2
- [41] Tao Yu, Zerong Zheng, Kaiwen Guo, Pengpeng Liu, Qionghai Dai, and Yebin Liu. Function4d: Real-time human volumetric capture from very sparse consumer rgbd sensors. In *IEEE Conference on Computer Vision and Pattern Recognition (CVPR2021)*, 2021. 3, 8
- [42] Juze Zhang, Haimin Luo, Hongdi Yang, Xinru Xu, Qianyang Wu, Ye Shi, Jingyi Yu, Lan Xu, and Jingya Wang. Neural-dome: A neural modeling pipeline on multi-view human-object interactions. In *CVPR*, 2023. 1, 2
- [43] Jason Y. Zhang, Sam Pepose, Hanbyul Joo, Deva Ramanan, Jitendra Malik, and Angjoo Kanazawa. Perceiving 3d human-object spatial arrangements from a single image in the wild. In *European Conference on Computer Vision (ECCV)*, 2020. 2
- [44] Xiaohan Zhang, Bharat Lal Bhatnagar, Sebastian Starke, Vladimir Guzov, and Gerard Pons-Moll. Couch: Towards controllable human-chair interactions. 2022. 3
- [45] Zerong Zheng, Tao Yu, Yebin Liu, and QiongHai Dai. Pamir: Parametric model-conditioned implicit representation for image-based human reconstruction, 2021. 1, 5